Electronic Supplementary Material (ESI) for Journal of Materials Chemistry A.

Electronic Supplementary Information

Mesoporous C-coated SnO_x nanosheets on copper foil as flexible and binder-free anodes for superior sodium-ion batteries

Haidong Bian[a,b], Xufen Xiao[a], Shanshan Zeng[a,c], Muk-Fung Yuen[a,c], Zebiao Li[c], Wenpei Kang[a,c], Denis Y.W.Yu[a], Zhengtao Xu[b,*], Jian Lu[d,e], Yang Yang Li[a,c,f,*]

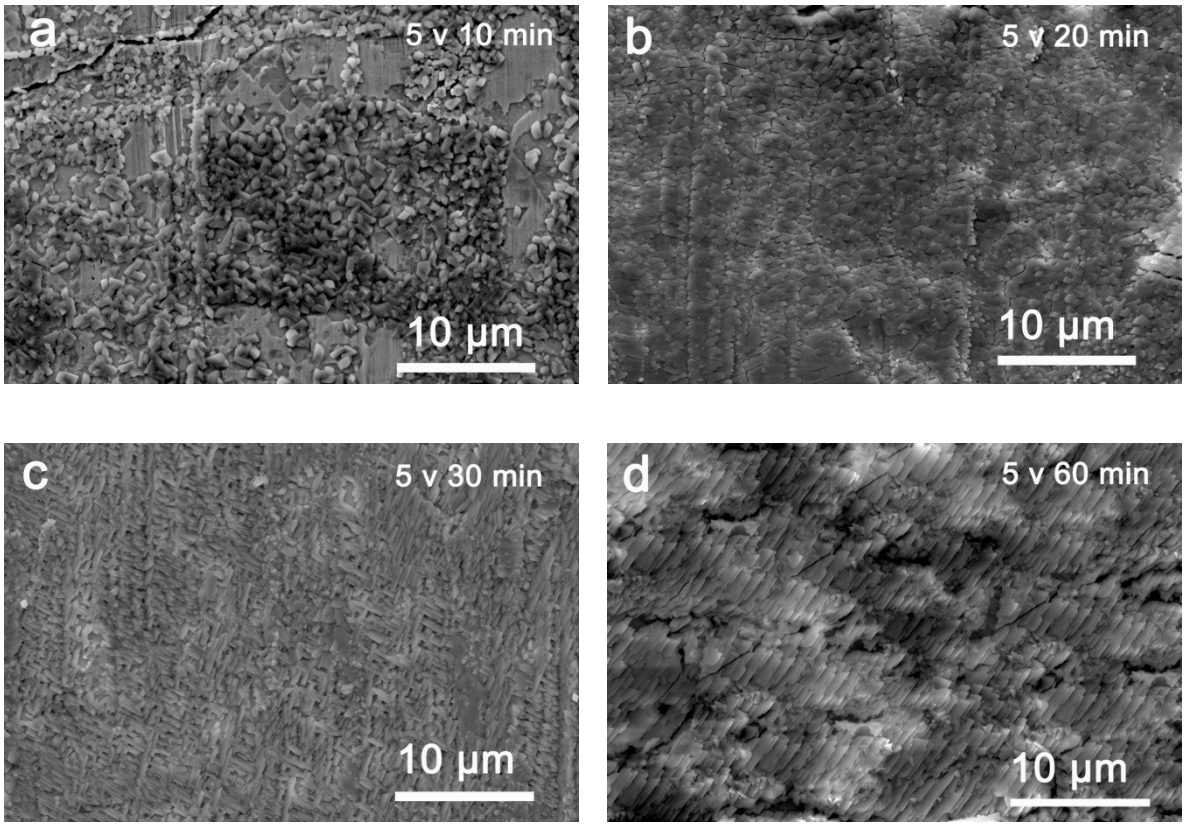

Figure S1. SEM images of the as-anodized tin foils treated in a glycerol (containing 3 vol.% H_2O) solution of 0.1 M NH_4F and 0.1 M $H_2C_2O_4$ at 5 V for different time durations: a) 10 min, b) 20 min, c) 30 min, d) 60 min, showing the growth process of the self-assembled anodic tin(II) acetate ($SnC_4H_6O_4$) nanosheets. It was observed that particles were first randomly formed and scattered on the surface after 10 min's anodization, which then became a continuous film at 20 min. Rectangular nanosheets of ~ 500 nm wide were observed at 30 min, which grew into a self-assembled nanosheets array at 60 min. The nucleation and growth of the anodic nanostructures observed here (in the glycerol electrolyte system) is similar to that observed in the ethylene glycol system previously reported by us.[1]

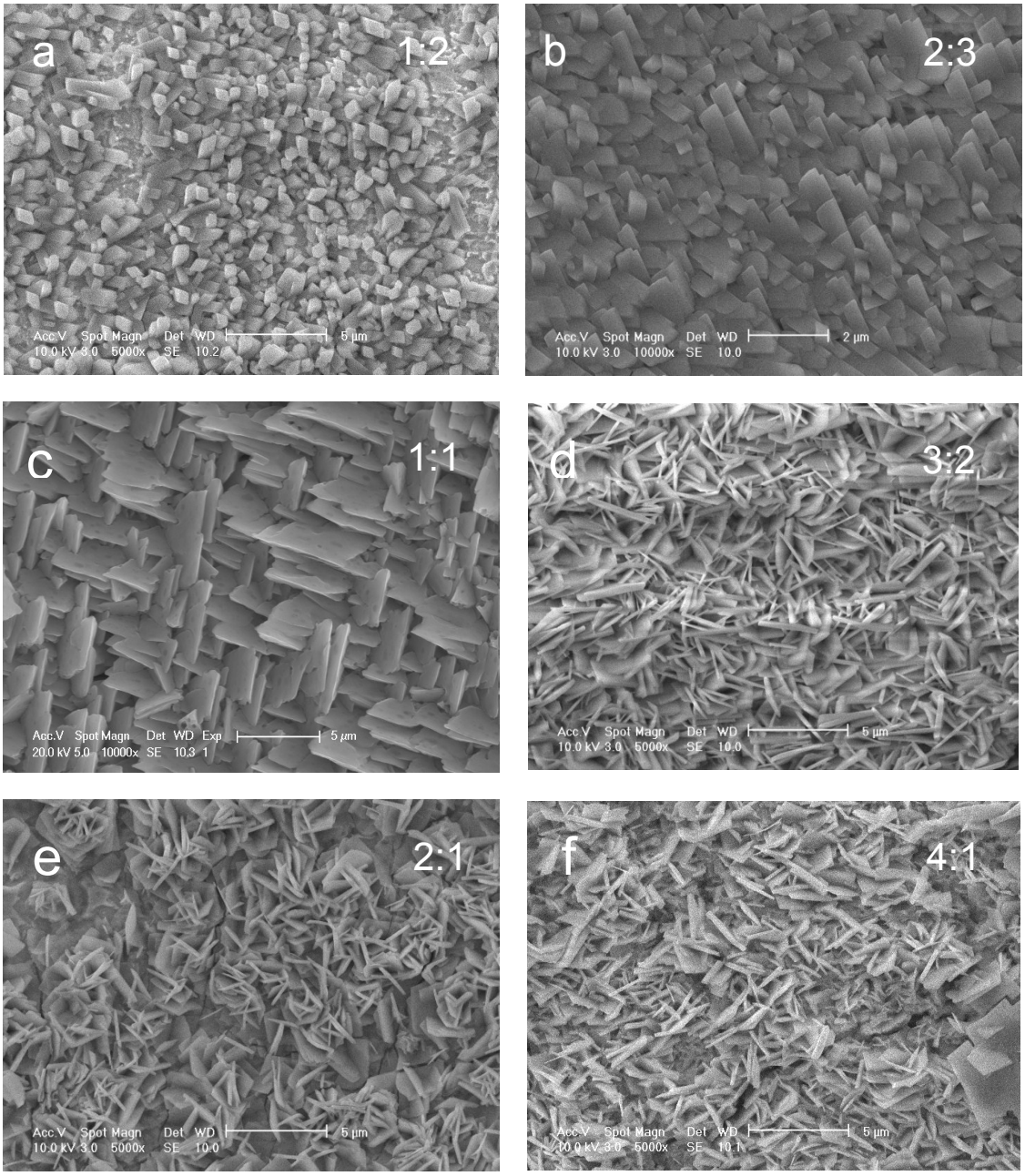

Figure S2. SEM images of tin substrate anodized at 5 V for 60 min in a glycerol (containing 3 vol% H_2O) solution of 0.1 M $H_2C_2O_4$ and different concentrations of NH_4F: a) 0.05M, b) 0.067 M, c) 0.1 M, d) 0.15 M, e) 0.2 M, and f) 0.4 M, showing the impact of the $F^-/C_2O_4^{2-}$ ratio on the anodic morphology obtained. With the $F^-/C_2O_4^{2-}$ ratio below 1, only granular films were obtained. By increasing the $F^-/C_2O_4^{2-}$ ratio above 1:1, self-assembled rectangular nanosheets were obtained with sheet width varying ~ 2 - 5 µm (d-f).

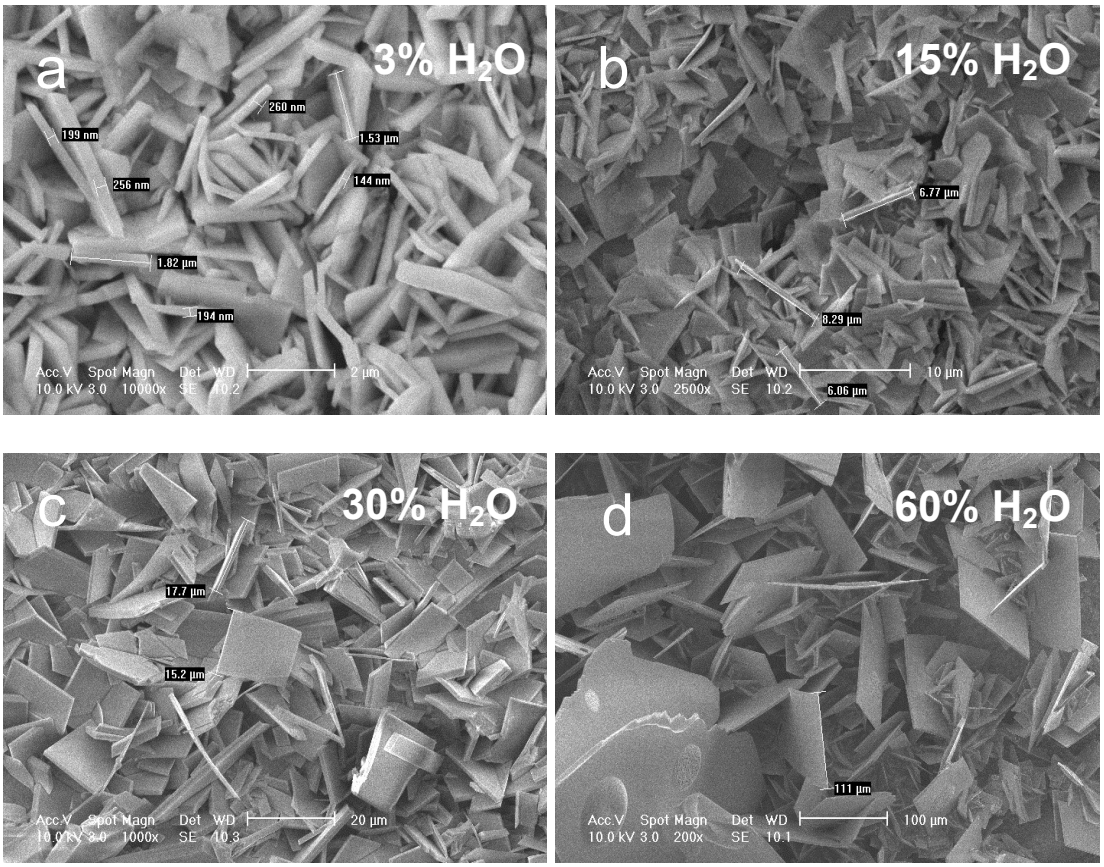

Figure S3. SEM images of the tin substrate anodized at 5 V for 60 min in the glycerol (containing 3 vol% (a), 15 vol% (b), 30 vol% (c), or 60 vol% (d) H_2O) solution of 0.1 M $H_2C_2O_4$ and 0.15 M of NH_4F. It can be seen that larger rectangular nanosheets were obtained with higher water content in glycerol (nanosheets size of ~ 1.5 to 150 µm for H_2O content of 3 to 60 vol%).

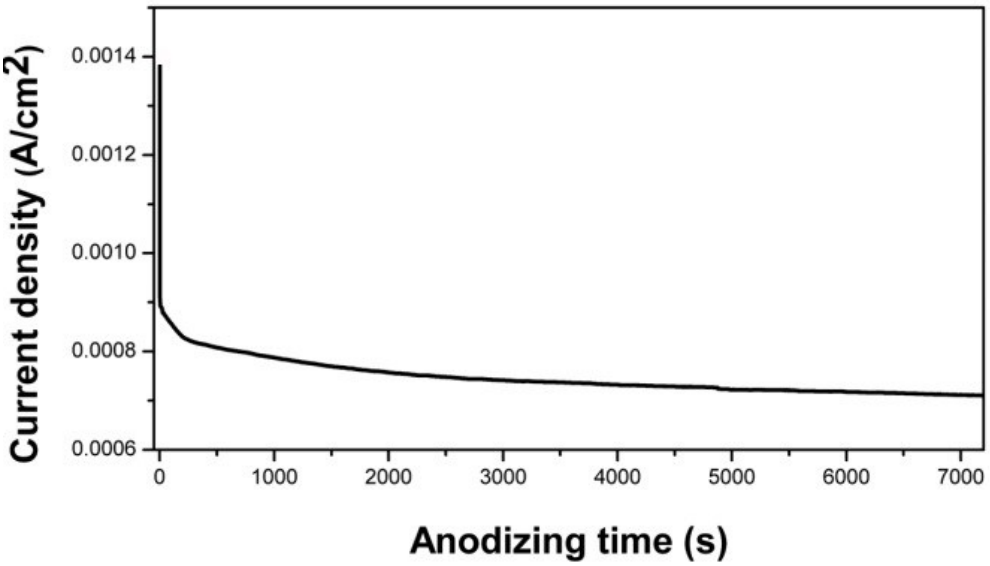

Figure S4. Typical current density *vs*. time (*i*-*t*) profile recorded for a pure Sn foil anodized at 5 V for 7200 s in a glycerol (containing 15 vol.% H_2O) solution of 0.2 M NH_4F and 0.1 M $H_2C_2O_4$.

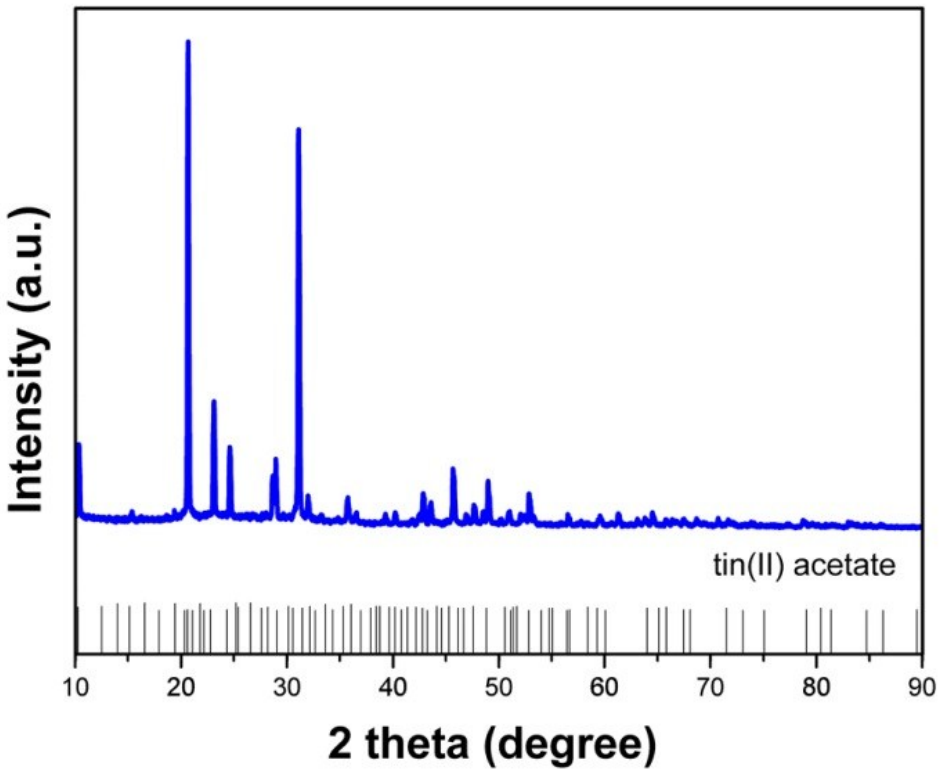

Figure S5. XRD pattern of the tin(II) acetate ($SnC_4H_6O_4$) nanosheets fabricated by anodization at 5 V for 3600 s in a glycerol (containing 15 vol.% H_2O) solution of 0.2 M NH_4F and 0.1 M $H_2C_2O_4$.

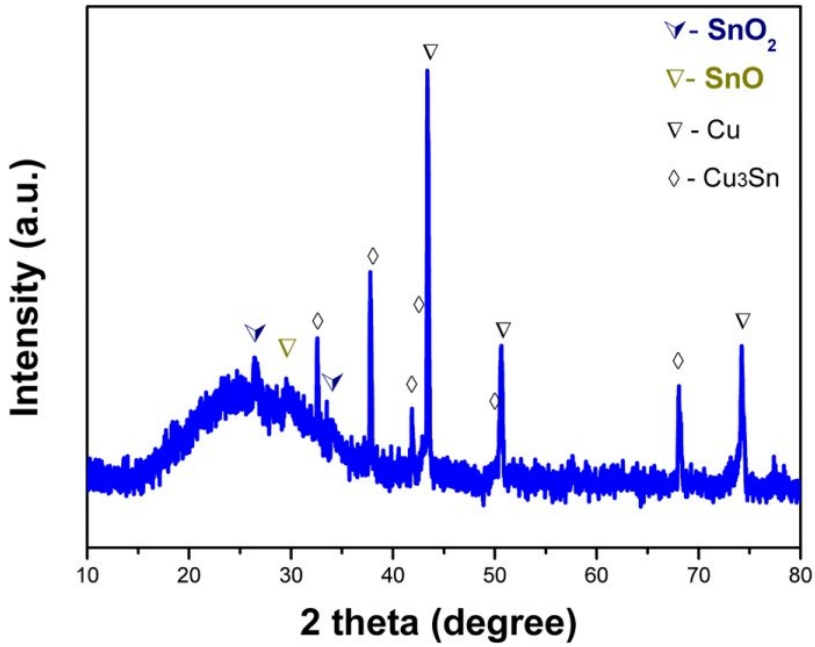

Figure S6. XRD pattern of the anodized sample after annealed at 300 ^{o}C for 2 h in Ar. The anodization was carried out at 5 V for 1800 s in a glycerol (containing 15 vol. % H_2O) solution of 0.2 M NH_4F and 0.1 M $H_2C_2O_4$.

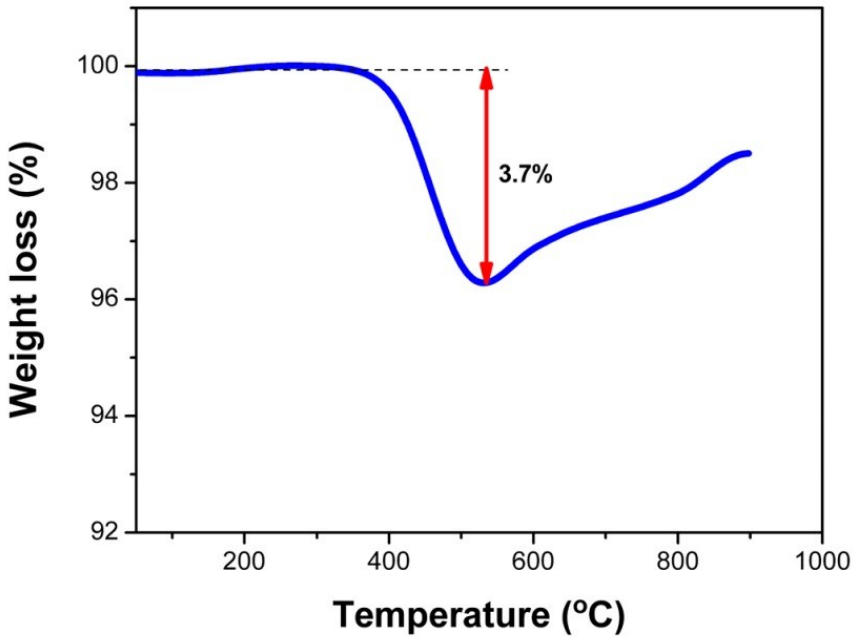

Figure S7. TGA curve of the C@SnO_x/Cu sample measured between 30 and 900 °C at a heating rate of 10 °C min^{-1} in air.

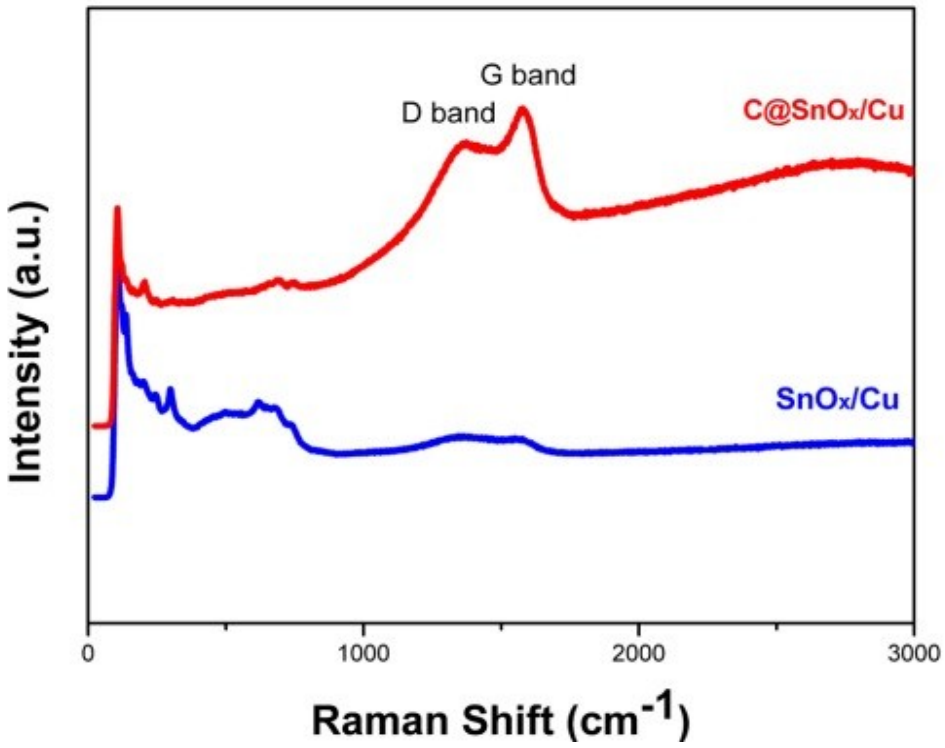

Figure S8. Raman spectra of as-fabricated SnO_x/Cu and C@SnO_x/Cu.

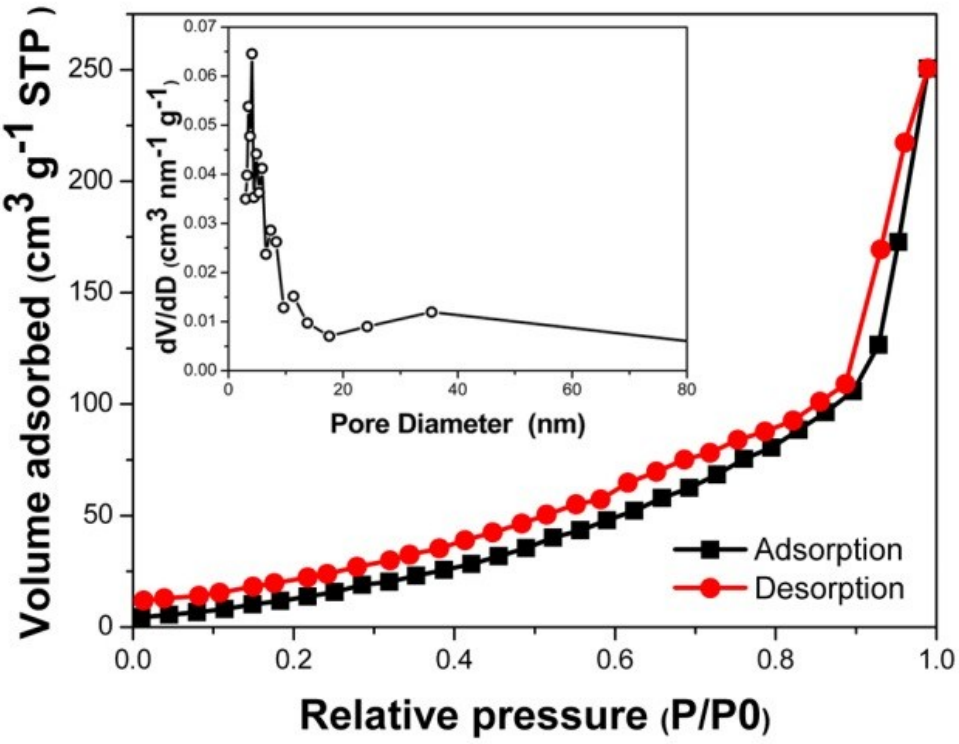

Figure S9. N_2 adsorption and desorption isotherms of porous SnO_x at 77 K with the inset showing the pore-size distribution calculated using the BJH method from the adsorption branch**.**

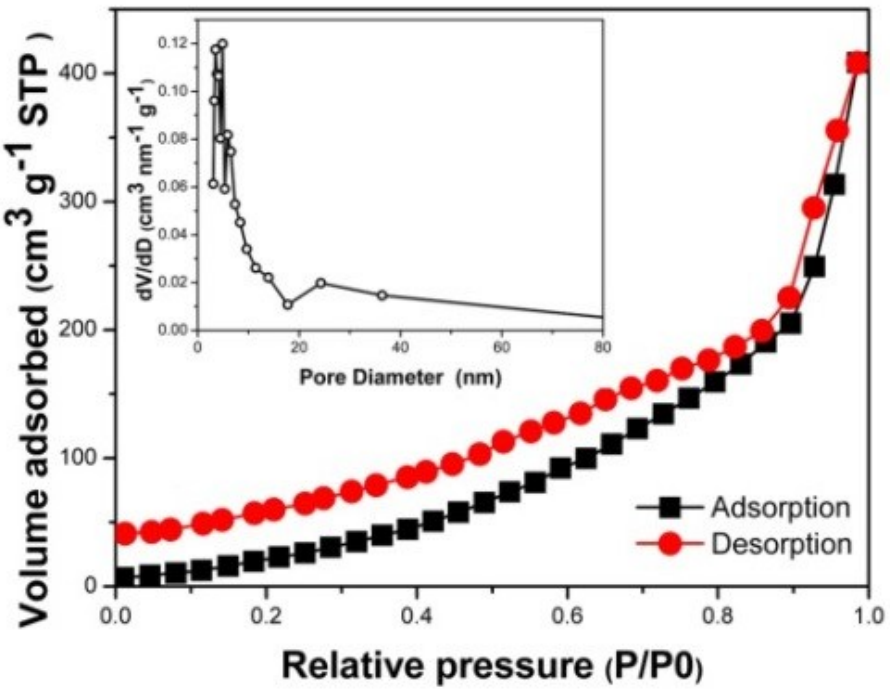

Figure S10. N_2 adsorption and desorption isotherms of as-prepared porous C@SnO_x at 77 K. The inset shows the pore-size distribution calculated from the adsorption branch using the BJH method**.**

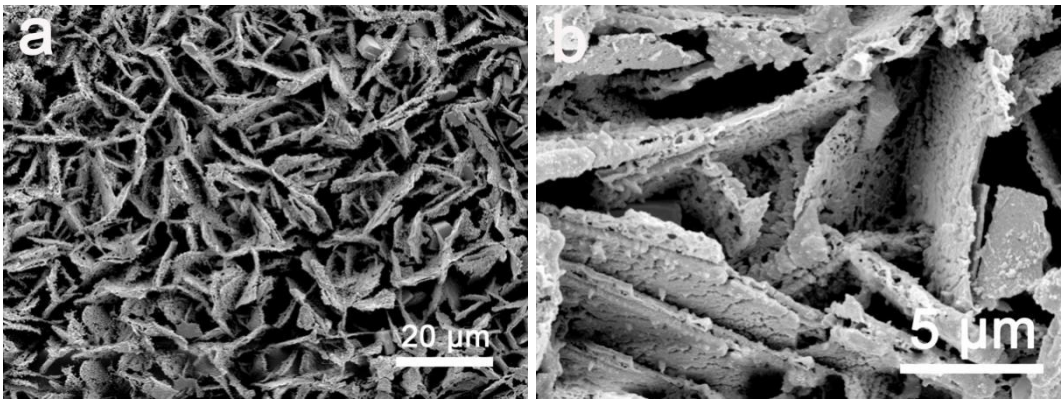

Figure S11. SEM images of as-annealed porous SnO_x sample (before carbon coating).

Table S1. Recent studies on SnO_2-based materials for NIBs.

Structure	Reversible capacity (mA h g^{-1})	Charge/discharge current density (mA g^{-1})	Cycles	Fabrication method	W/ binder?	Ref.
Mesoporous SnO_x nanosheets	404	100	100	facile anodization method	N	This work
Octahedral SnO_2 nanocrystals	432	20	100	hydrothermal method	Y	[2]
SnO_2@graphene	270	100	100	ball milling method	Y	[3]
SnO_2-RGO	330	100	150	hydrothermal method	Y	[4]
SnO_2@3DG	432	100	200	hydrothermal method	Y	[5]
WNTs@SnO_2 @C	200	150	300	hydrothermal method	Y	[6]
Al_2O_3/SnO_2/CC	375	134	100	hydrothermal and ALD method	N	[7]
A-SnO_2/CNT	223.2	1600	300	solution-based precipitation method	Y	[8]
PCNF@SnO_2 @C	374	50	100	electrodeposition	Y	[9]
SnO_2@void@C	401	50	50	Precipitation and heat treatment	Y	[10]
Sn/SnO_2/C	245	20	100	hydrothermal method	Y	[11]
Mesoporous Sn/SnO_2	372.3	50	50	temptation method	Y	[12]
a-SnO_2/GA	380.2	50	100	hydrothermal method	Y	[13]
SnO_2 NRs/G	200	20	100	hydrothermal method	Y	[14]

SnO_2/C	238	50	50	hydrothermal method	Y	[15]
Mesoporous C@SnO_x nanosheets	510	100	100	facile anodization followed by carbonization	N	This work

Reference

[1]. Bian, H.; Tian, Y.; Lee, C.; Yuen, M.-F.; Zhang, W.; Li, Y. Y., *ACS Appl. Mat. Interfaces* **2016,** *8*, 28862-28871.

[2]. Su, D.; Wang, C.; Ahn, H.; Wang, G., *PCCP* **2013,** *15*, 12543-12550.

[3]. Li, S.; Wang, Y.; Qiu, J.; Ling, M.; Wang, H.; Martens, W.; Zhang, S., *RSC Adv.* **2014,** *4*, 50148-50152.

[4]. Wang, Y.-X.; Lim, Y.-G.; Park, M.-S.; Chou, S.-L.; Kim, J. H.; Liu, H.-K.; Dou, S.-X.; Kim, Y.-J., *J. Mater. Chem. A* **2014,** *2*, 529-534.

[5]. Pei, L.; Jin, Q.; Zhu, Z.; Zhao, Q.; Liang, J.; Chen, J., *Nano Res.* **2015,** *8*, 184-192.

[6]. Zhao, Y.; Wei, C.; Sun, S.; Wang, L. P.; Xu, Z. J., *Advanced Science* **2015,** *2*, 1500097.

[7]. Liu, Y.; Fang, X.; Ge, M.; Rong, J.; Shen, C.; Zhang, A.; Enaya, H. A.; Zhou, C., *Nano Energy* **2015,** *16*, 399-407.

[8]. Cui, J.; Xu, Z.-L.; Yao, S.; Huang, J.; Huang, J.-Q.; Abouali, S.; Garakani, M. A.; Ning, X.; Kim, J.-K., *J. Mater. Chem. A* **2016,** *4*, 10964-10973.

[9]. Dirican, M.; Lu, Y.; Ge, Y.; Yildiz, O.; Zhang, X., *ACS Appl. Mat. Interfaces* **2015,** *7*, 18387-

18396.

[10]. Li, H. Z.; Yang, L. Y.; Liu, J.; Li, S. T.; Fang, L. B.; Lu, Y. K.; Yang, H. R.; Liu, S. L.; Lei, M., *J. Power Sources* **2016,** *324*, 780-787.

[11]. Cheng, Y.; Huang, J.; Li, J.; Xu, Z.; Cao, L.; Qi, H., *J. Power Sources* **2016,** *324*, 447-454.

[12]. Tang, D.; Huang, Q.; Yi, R.; Dai, F.; Gordin, M. L.; Hu, S.; Chen, S.; Yu, Z.; Sohn, H.; Song, J.; Wang, D., *Eur. J. Inorg. Chem.* **2016,** *2016*, 1950-1954.

[13]. Fan, L.; Li, X.; Yan, B.; Feng, J.; Xiong, D.; Li, D.; Gu, L.; Wen, Y.; Lawes, S.; Sun, X., *Adv. Energy Mater.* **2016,** *6*, 1502057.

[14]. Zhu, J.; Deng, D., *Chem. Eng. Sci.* **2016,** *154*, 54-60.

[15]. Lu, Y. C.; Ma, C.; Alvarado, J.; Kidera, T.; Dimov, N.; Meng, Y. S.; Okada, S., *J. Power Sources* **2015,** *284*, 287-295.